



20 Oct 2016

Polymer-Coated Therapeutic Nanoparticles

Sutapa Barua

Missouri University of Science and Technology, baruas@mst.edu

Follow this and additional works at: https://scholarsmine.mst.edu/che_bioeng_facwork

 Part of the [Chemical Engineering Commons](#)

Recommended Citation

S. Barua, "Polymer-Coated Therapeutic Nanoparticles," *U.S. Patents*, Oct 2016.

This Patent is brought to you for free and open access by Scholars' Mine. It has been accepted for inclusion in Chemical and Biochemical Engineering Faculty Research & Creative Works by an authorized administrator of Scholars' Mine. This work is protected by U. S. Copyright Law. Unauthorized use including reproduction for redistribution requires the permission of the copyright holder. For more information, please contact scholarsmine@mst.edu.



US 20160303053A1

(19) **United States**

(12) **Patent Application Publication**
Barua

(10) **Pub. No.: US 2016/0303053 A1**

(43) **Pub. Date: Oct. 20, 2016**

(54) **POLYMER-COATED THERAPEUTIC NANOPARTICLES**

Publication Classification

(71) Applicant: **Sutapa Barua**, Rolla, MO (US)

(51) **Int. Cl.**
A61K 9/51 (2006.01)
A61K 31/4745 (2006.01)
A61K 47/48 (2006.01)

(72) Inventor: **Sutapa Barua**, Rolla, MO (US)

(52) **U.S. Cl.**
CPC *A61K 9/5153* (2013.01); *A61K 9/5192* (2013.01); *A61K 47/48884* (2013.01); *A61K 31/4745* (2013.01); *A61K 47/48584* (2013.01)

(21) Appl. No.: **15/130,544**

(22) Filed: **Apr. 15, 2016**

(57) **ABSTRACT**
Polymer-coated therapeutic nanoparticles, methods of making and using the same are provided. The polymer-coated therapeutic nanoparticles can include an inner core having at least one therapeutic agent and an outer polymeric coating covering at least a portion of the inner core. A targeting molecule can be associated with the outer polymeric coating.

Related U.S. Application Data

(60) Provisional application No. 62/178,647, filed on Apr. 15, 2015.

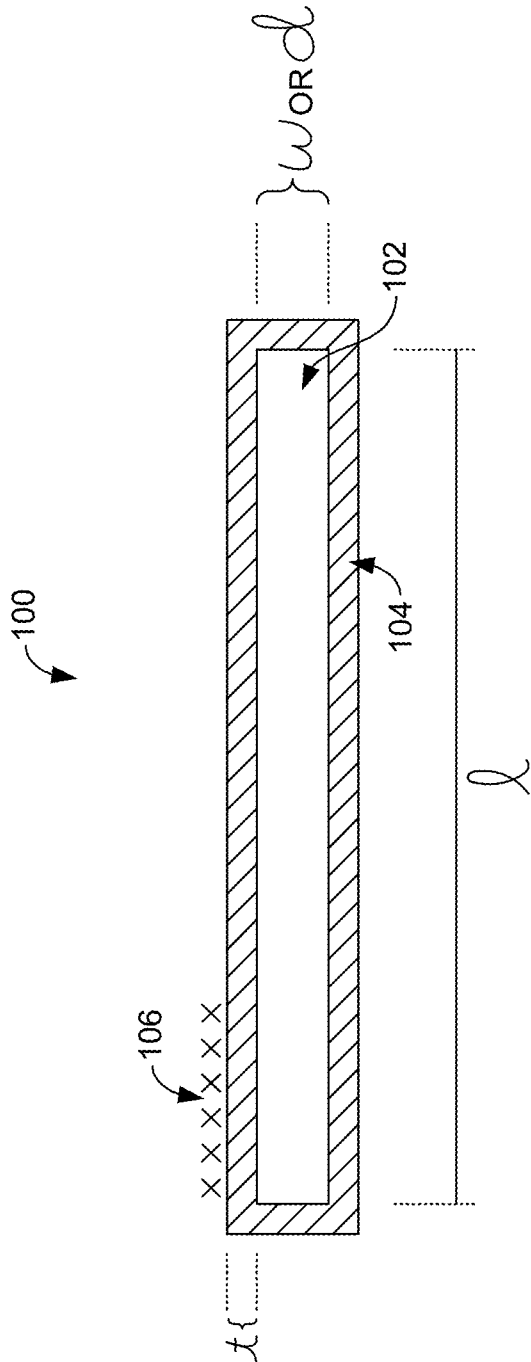


FIG. 1.

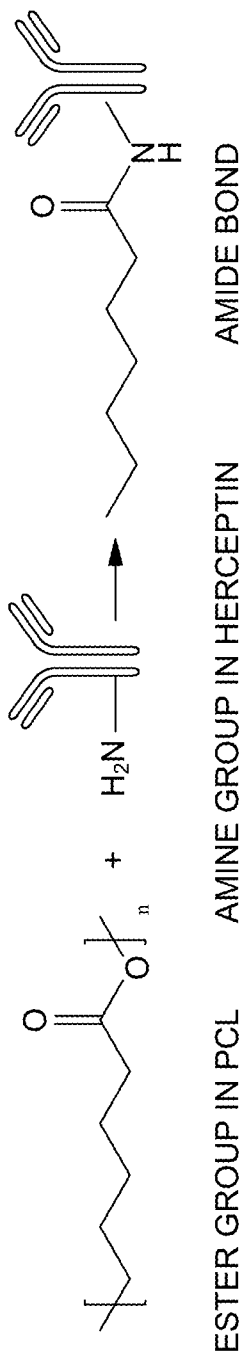


FIG. 2.

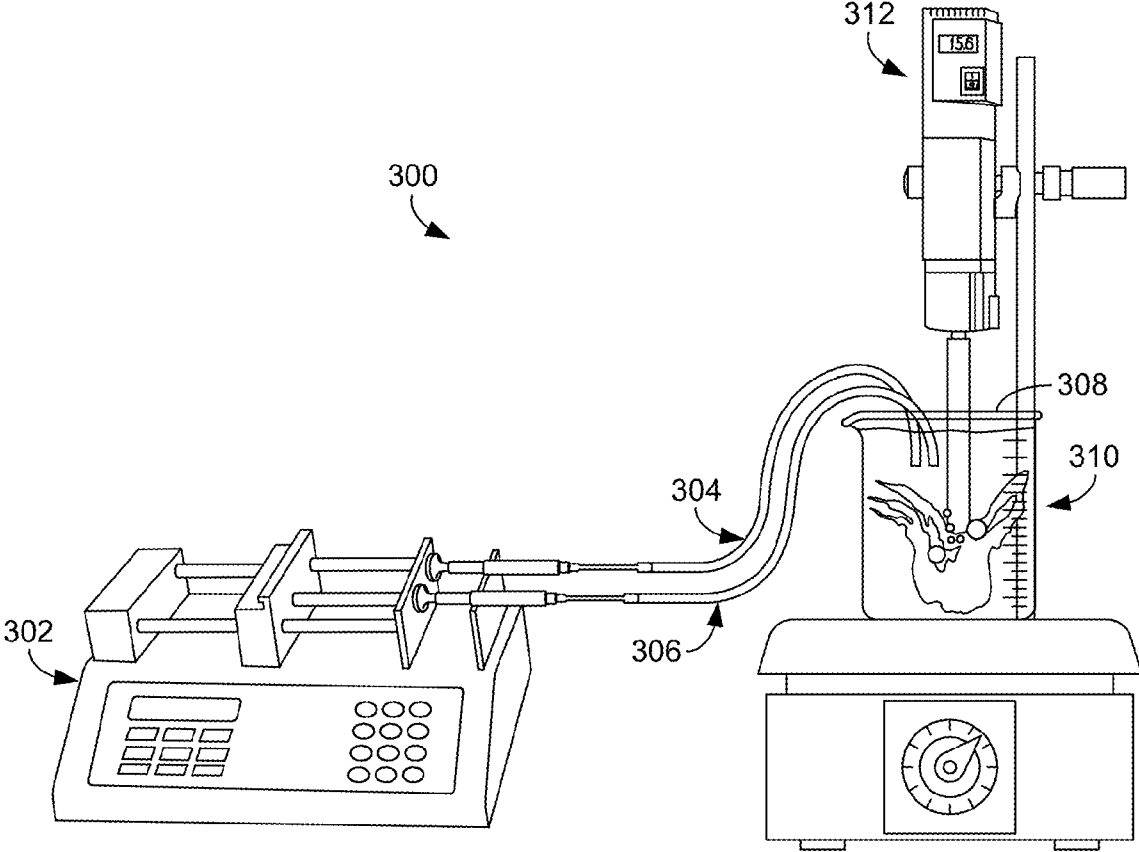


FIG. 3.

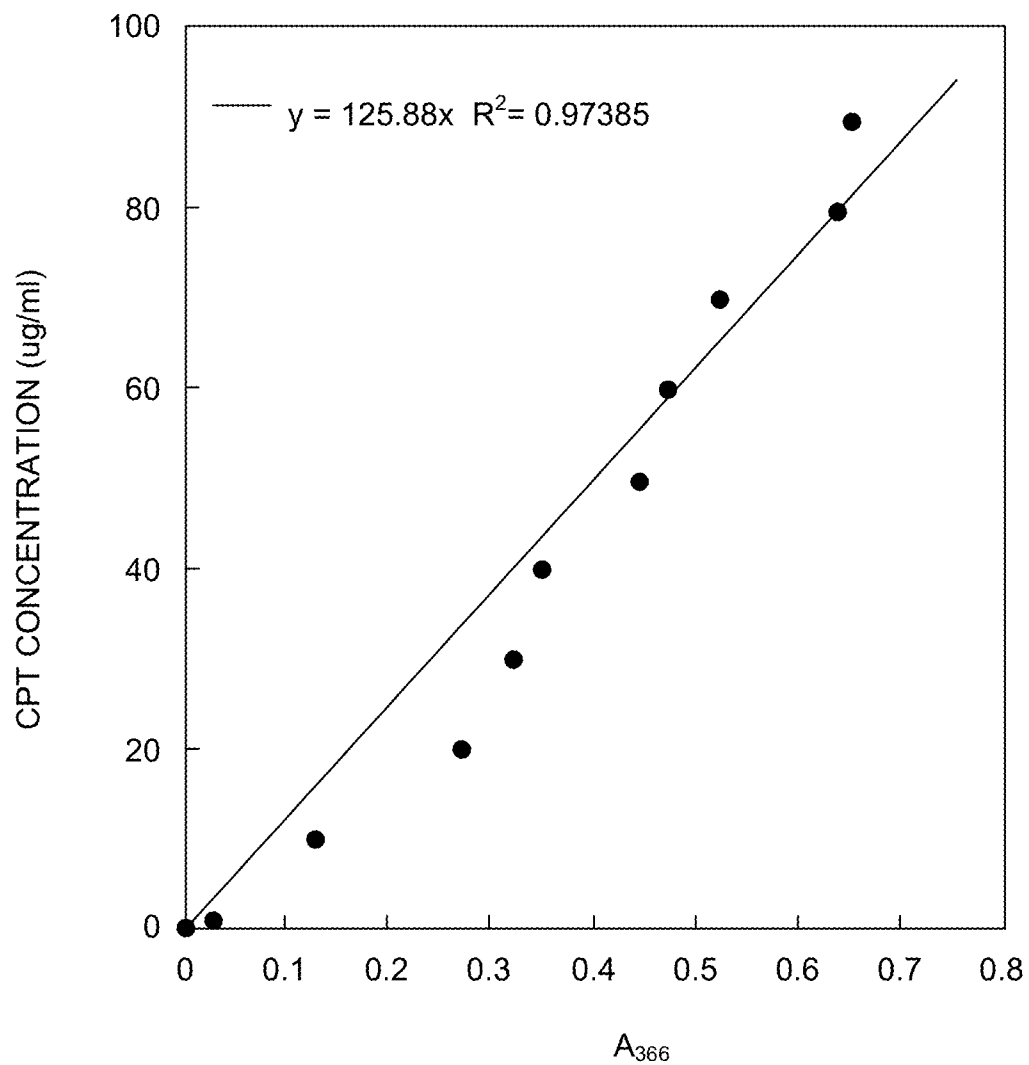


FIG. 4.

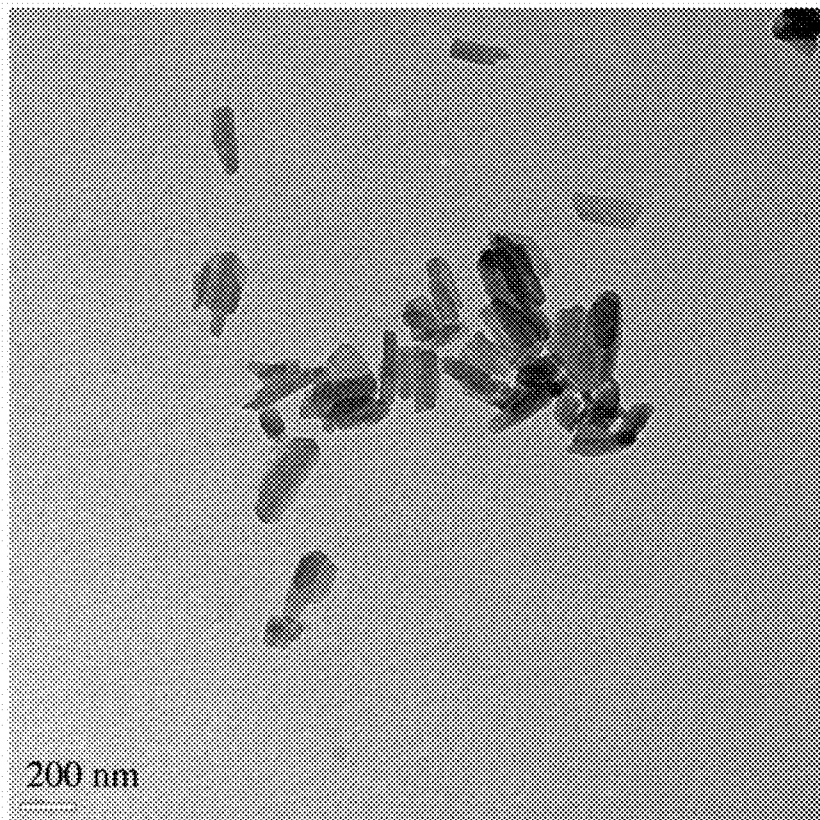


FIG. 5A.

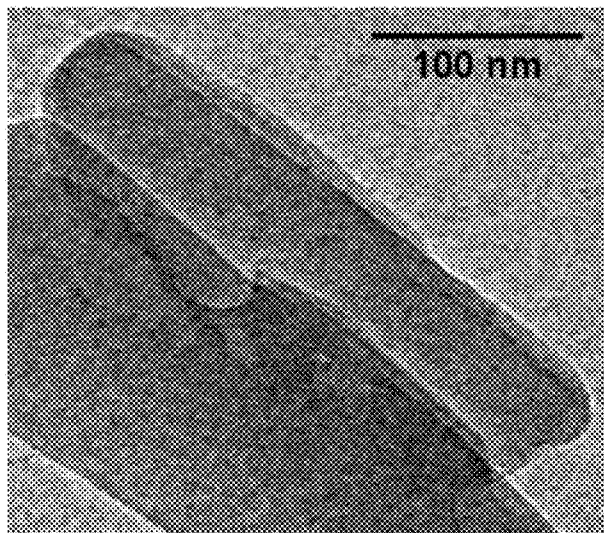


FIG. 5B.

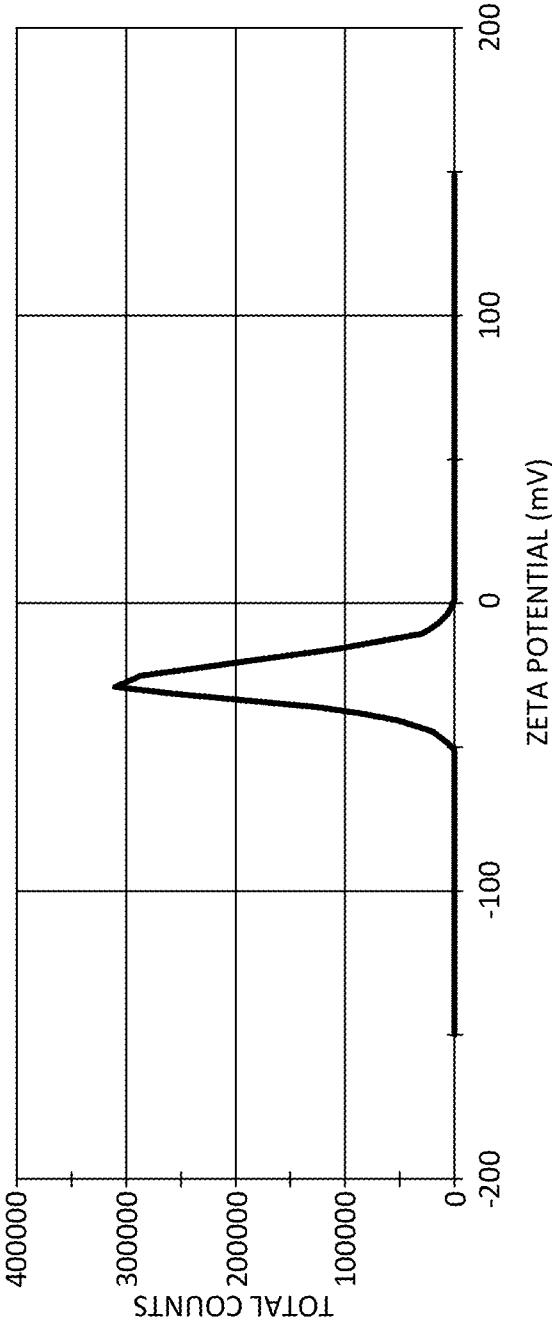


FIG. 6A.

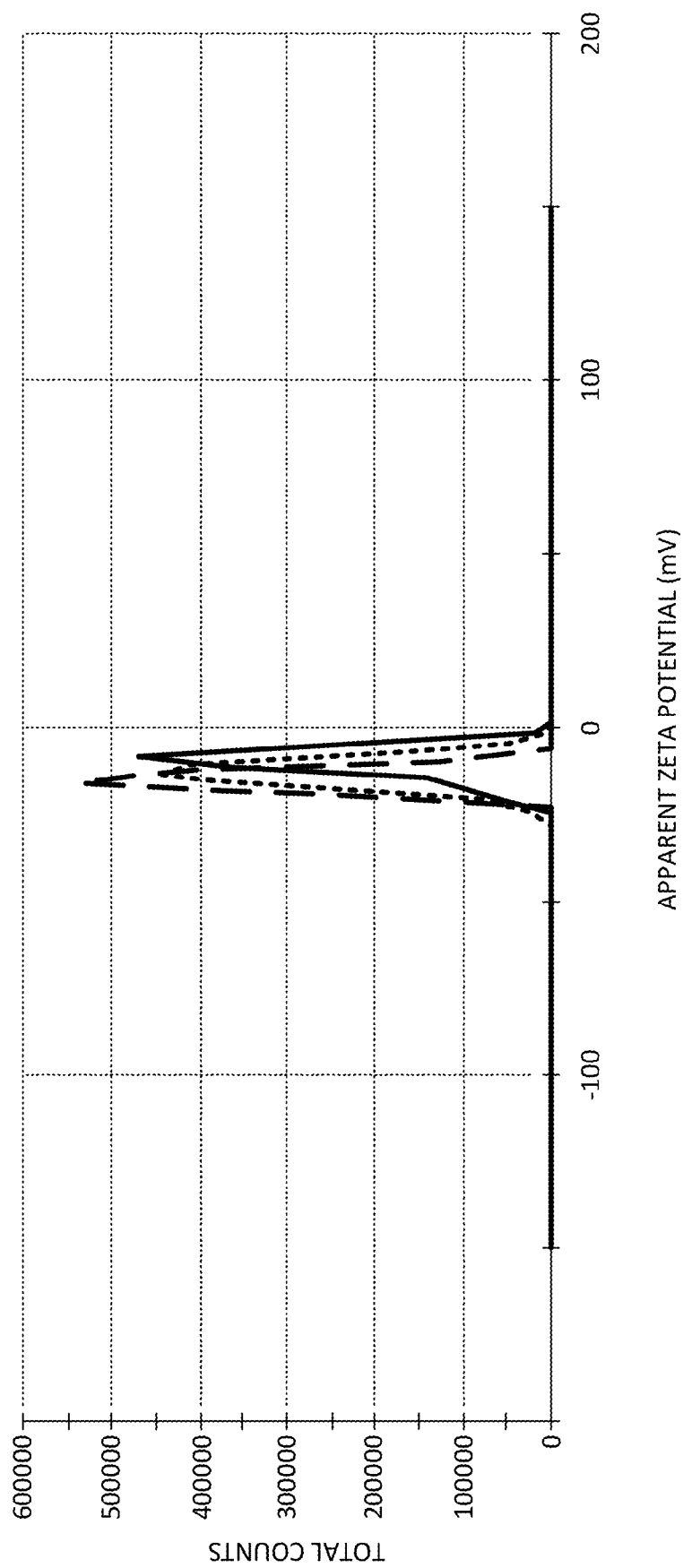


FIG. 6B.

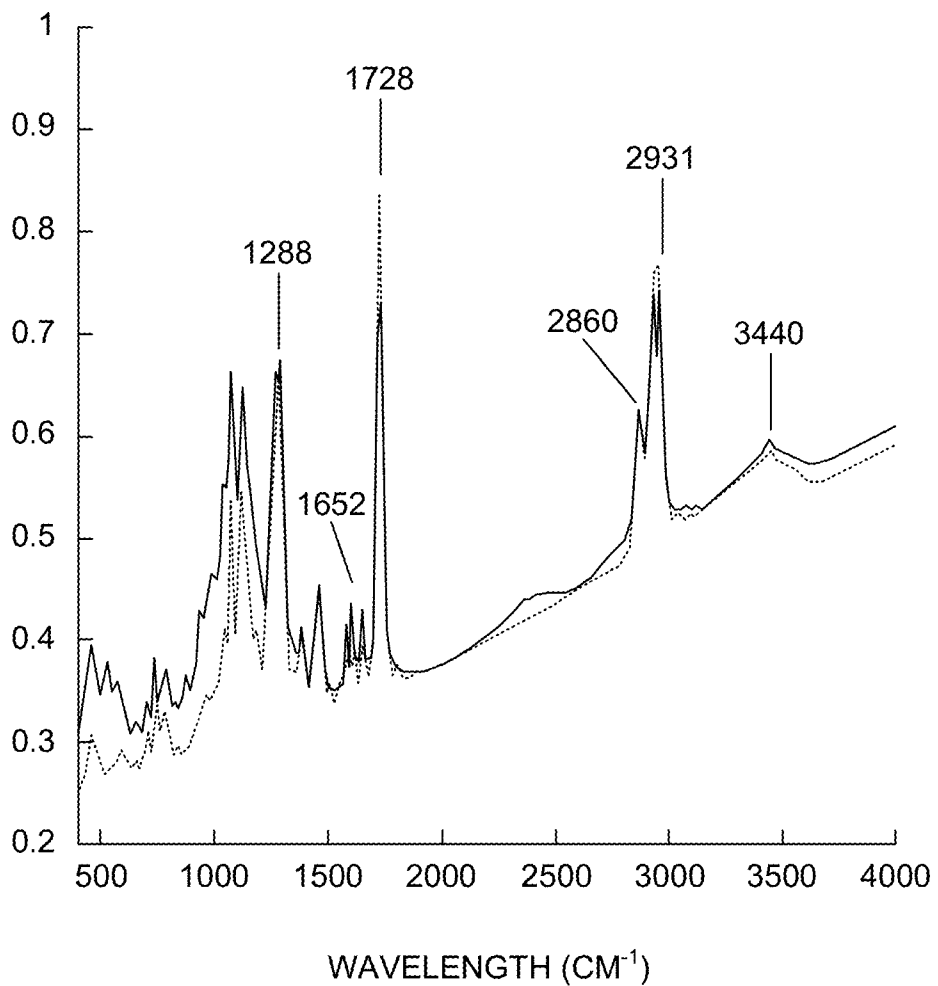


FIG. 7.

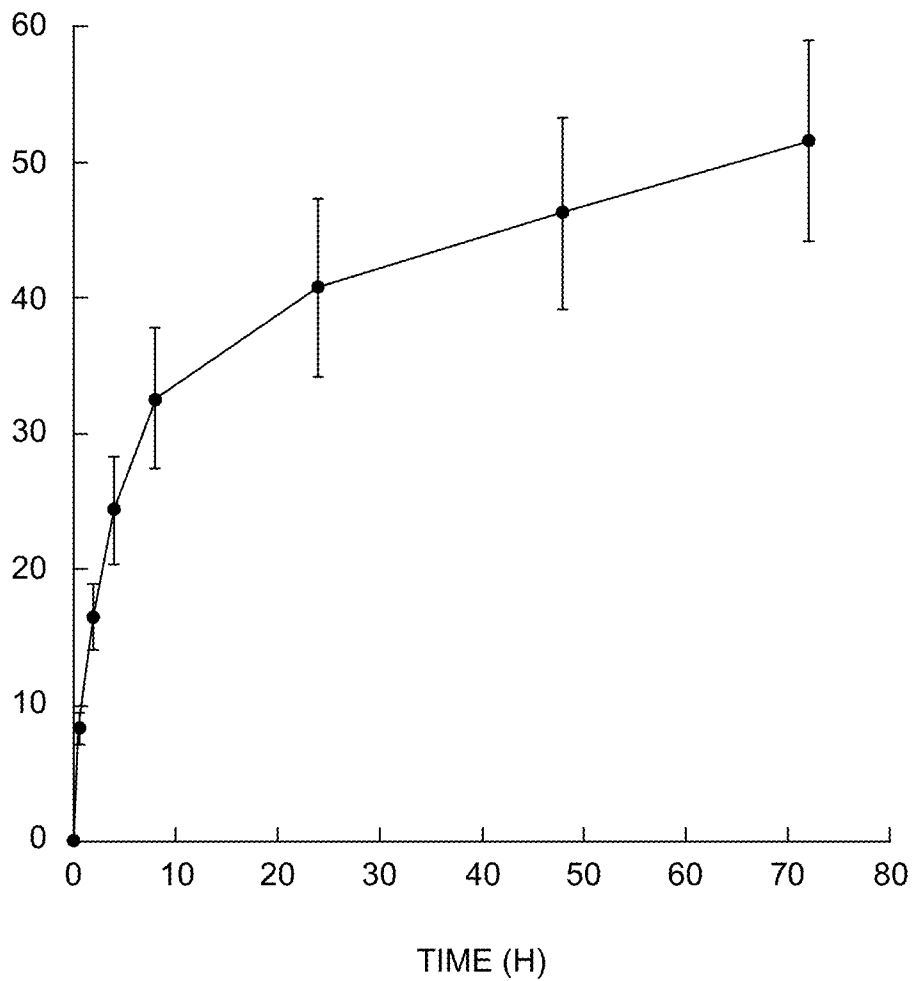


FIG. 8A.

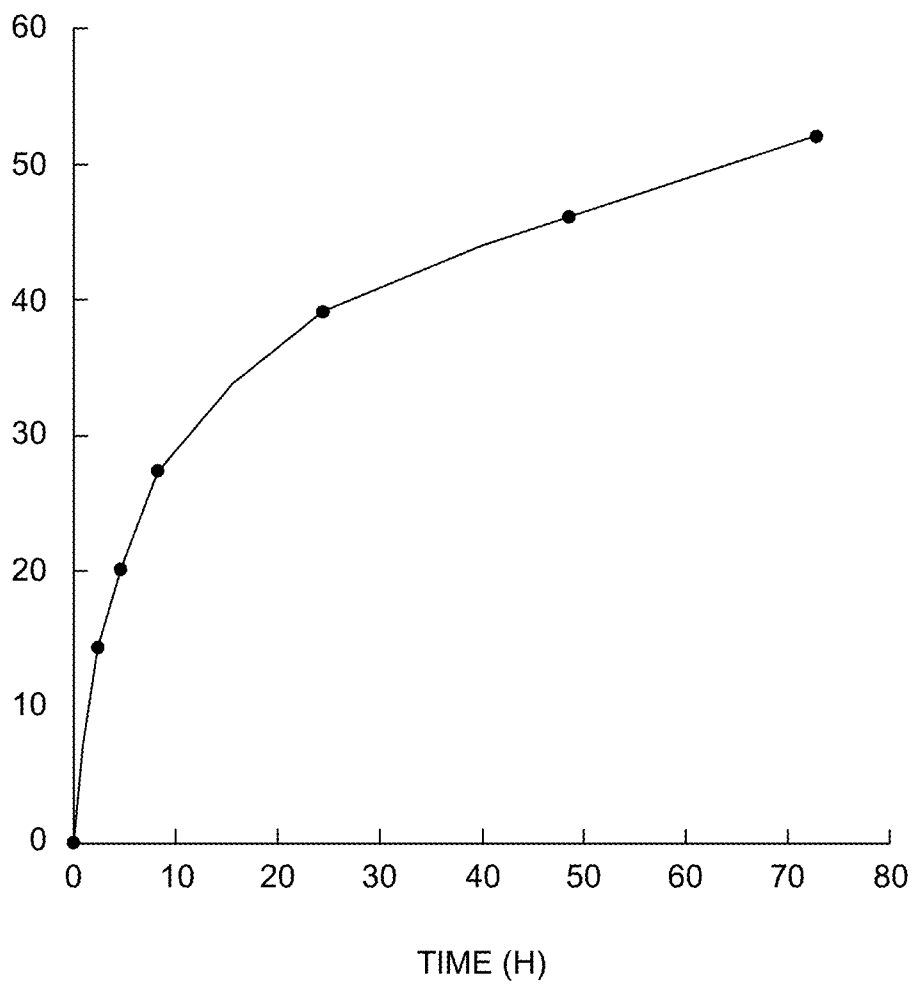


FIG. 8B.

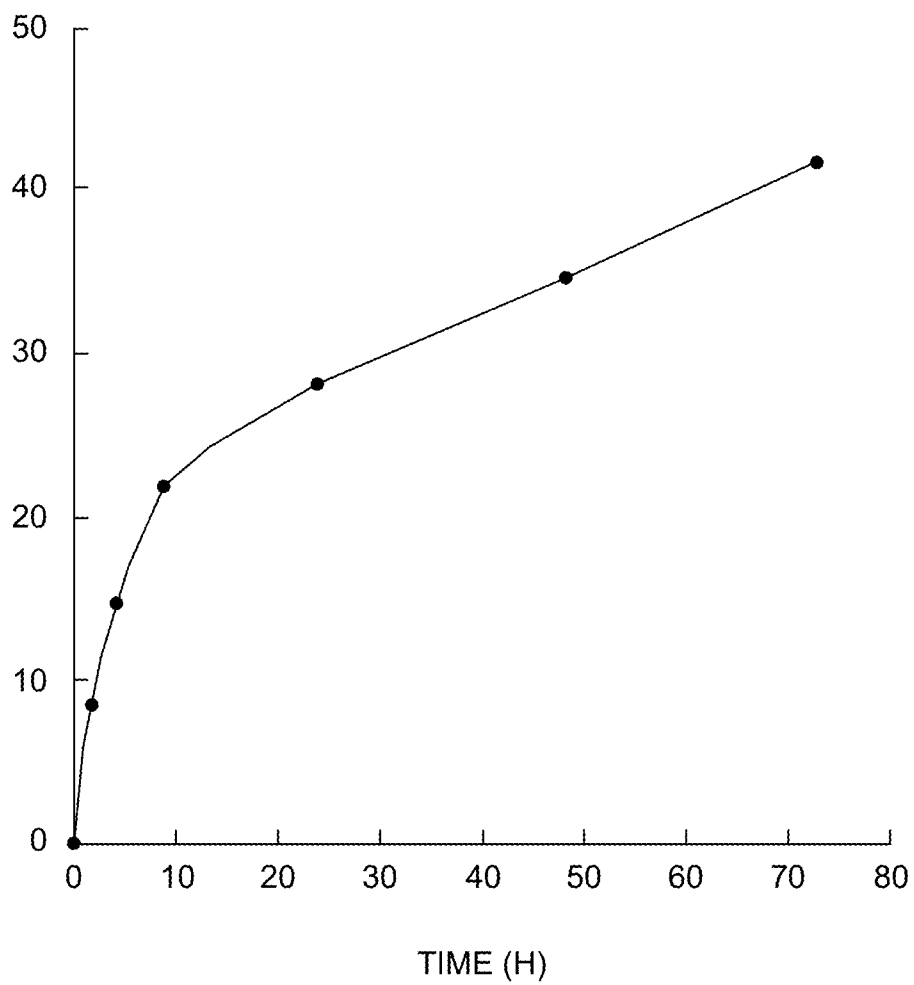


FIG. 8C.

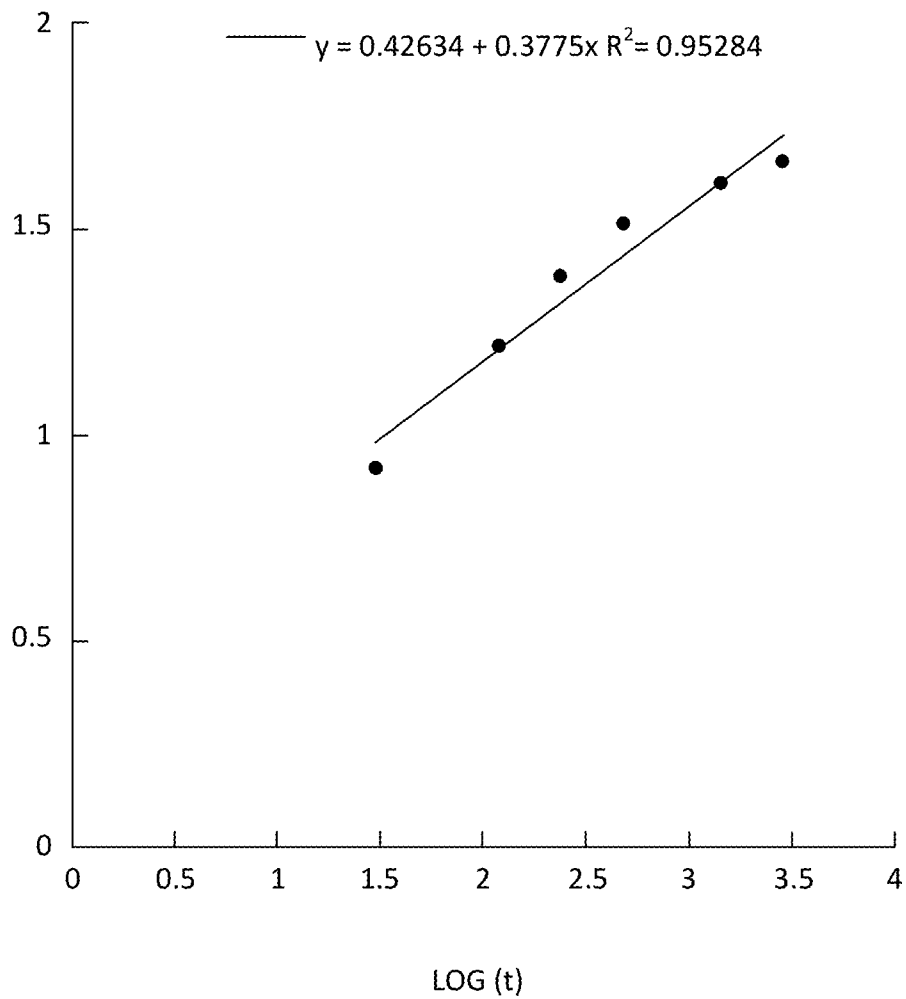


FIG. 9.

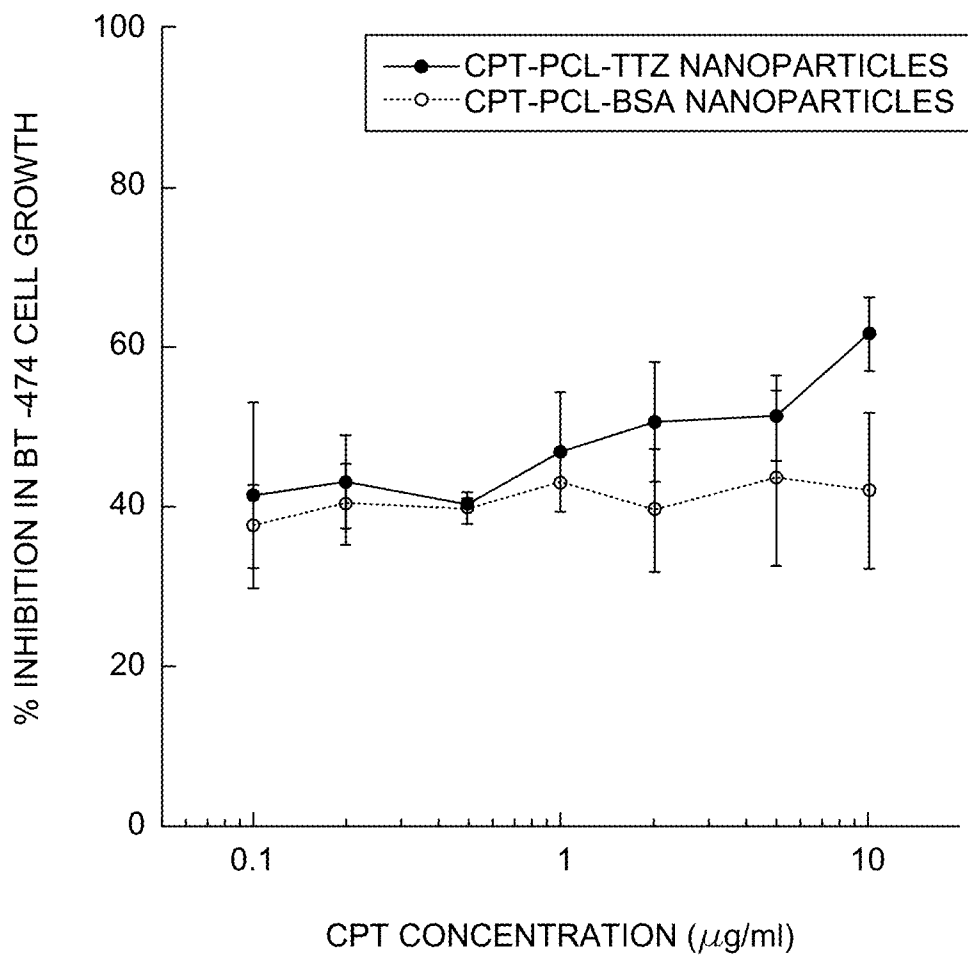


FIG. 10.

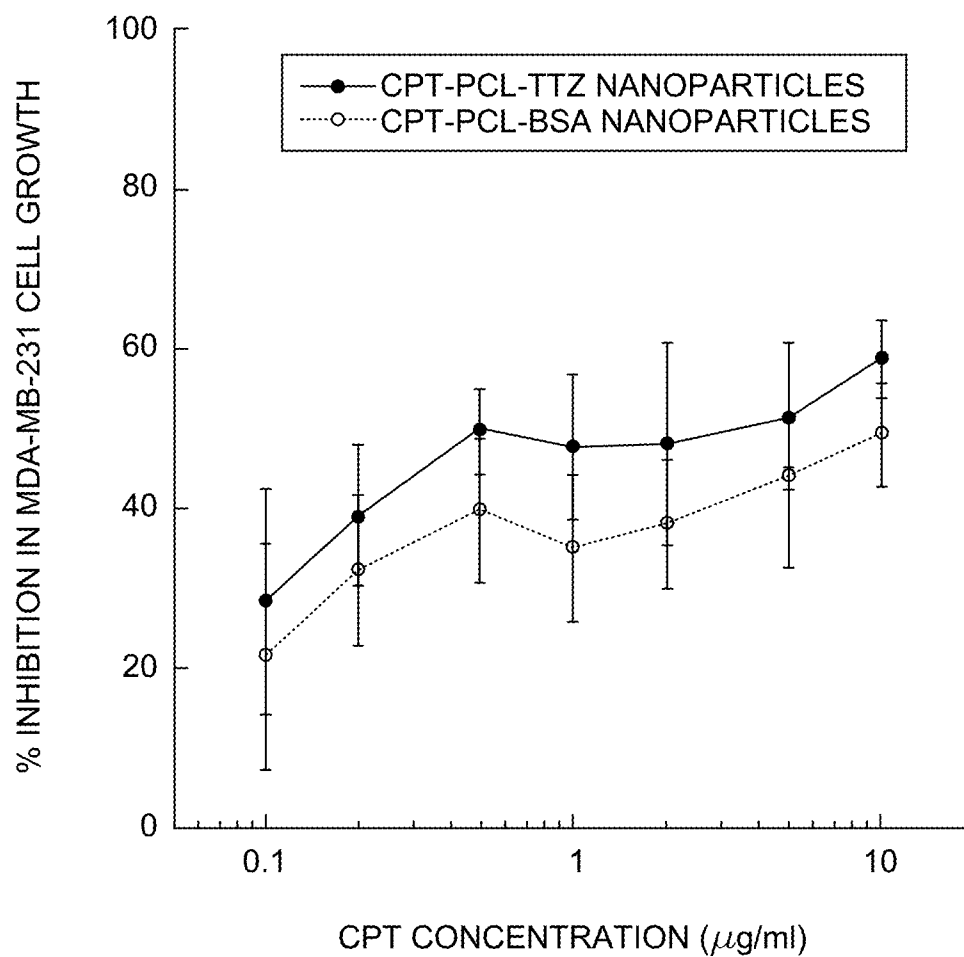
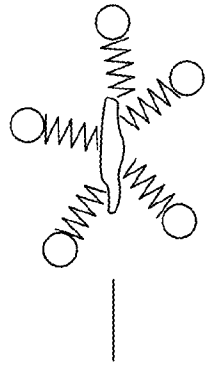
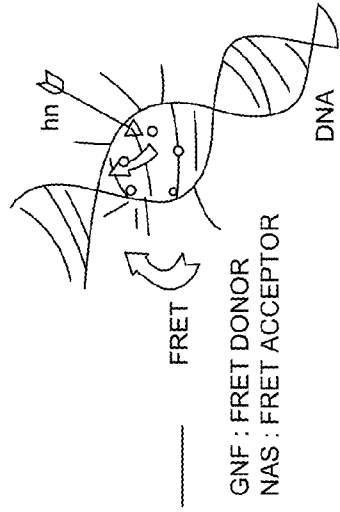


FIG. 11.



GNF-NAS CONJUGATE

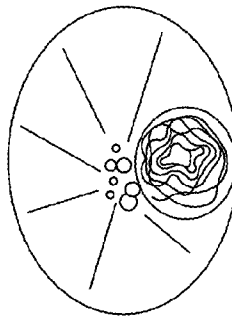


GLASS NANOFIBER (GNF) + NUCLEIC ACID STAIN (NAS)



GLASS NANOFIBER (GNF)

NORMAL CELLS CONTAIN 2N NUMBER OF DNA



GNF-NAS PROBE WILL BE USED TO STAIN THE DNA OF CANCER CELLS FOR THE EARLY DETECTION

CANCER CELLS HAVE ABNORMAL NUMBER (>2N) OF DNA

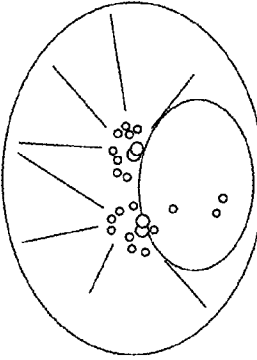


FIG. 12.

POLYMER-COATED THERAPEUTIC NANOPARTICLES

CROSS-REFERENCE TO RELATED APPLICATIONS

[0001] This application claims priority to U.S. Provisional Application Ser. No. 62/178,647 entitled "POLYMERIC NANOPARTICLES FOR DRUG DELIVERY AND BACTERIAL TOXIN REMOVAL," filed Apr. 15, 2015, the disclosure of which is hereby incorporated by reference as if set forth in its entirety herein.

FIELD

[0002] Therapeutic agents and methods of making and using the same are provided.

BACKGROUND

[0003] While there are a number of effective therapeutic compounds for the treatment of a number of diseases, such as cancer, there are some challenges to effectively delivering such therapeutic compounds to the intended target site. Certain current drug delivery methods and systems can result in the degradation of the therapeutic compound prior to its arrival at the target site. Further, simply increasing the dosage to deliver an effective amount of the therapeutic agent to the target site may not be possible, as in certain scenarios, such dosages may be toxic or cause other deleterious side effects.

SUMMARY

[0004] In one aspect, a polymer-coated therapeutic nanoparticle is provided. The polymer-coated therapeutic nanoparticle includes an inner core including at least one therapeutic agent. The inner core has a maximum dimension of 300 nm or less. The polymer-coated therapeutic nanoparticle also includes an outer polymeric coating that coats at least a portion of the inner core, wherein the outer polymeric coating has a thickness of 1 nm to 100 nm.

[0005] In another aspect, a method for producing a polymer-coated therapeutic nanoparticle is provided. The method includes forming an inner core including at least one therapeutic agent. The inner core has a maximum dimension of 300 nm or less. The method also includes coating, at least partly, the inner core with a layer of a bio-responsive polymer. The layer of the bio-responsive polymer has a thickness of 1 nm to 100 nm. The method further includes attaching at least one targeting molecule to the layer of the bio-responsive polymer.

[0006] In yet another aspect, a polymer-coated therapeutic nanoparticle. The polymer-coated therapeutic nanoparticle includes a rod-shaped inner core. The rod-shaped inner core includes an anti-cancer therapeutic agent. The rod-shaped inner core has a maximum dimension of 450 nm or less. The polymer-coated therapeutic nanoparticle also includes an outer polymeric coating at least partly covering the rod-shaped inner core. The outer polymeric coating has a thickness from 1 nm to 100 nm. The outer polymeric coating includes a bio-responsive polymer. The polymer-coated therapeutic nanoparticle also includes at least one targeting molecule covalently attached to the outer polymeric coating, wherein the at least one targeting molecule comprises a polypeptide.

BRIEF DESCRIPTION OF THE SEVERAL VIEWS OF THE DRAWINGS

[0007] The present invention is described in detail below with reference to the attached drawing figures, wherein:

[0008] FIG. 1 is a cross-sectional schematic view of a polymer-coated therapeutic nanoparticle, according to an aspect of the invention;

[0009] FIG. 2 is a schematic representation of a conjugation reaction for covalently attaching a targeting molecule to a polymer in the outer polymeric coating of a polymer-coated therapeutic nanoparticle, according to an aspect of the invention;

[0010] FIG. 3 is a perspective view of an exemplary solvent diffusion system for making polymer-coated therapeutic nanoparticles, according to an aspect of the invention;

[0011] FIG. 4 is a calibration curve for the concentration of camptothecin (CPT) at various absorbance values at 366 nm, according to an aspect of the invention;

[0012] FIG. 5A is a transmission electron microscopy (TEM) image of a sample of polymer-coated therapeutic nanoparticles that were produced as described in Example 1, according to an aspect of the invention;

[0013] FIG. 5B is a close-up TEM image of a sample of polymer-coated therapeutic nanoparticles that were produced as described in Example 1, according to an aspect of the invention;

[0014] FIG. 6A is a zeta potential distribution curve for CPT nanoparticles without a PCL polymer coating, as described in Example 2, in accordance with an aspect of the invention;

[0015] FIG. 6B is a zeta potential distribution curve for PCL polymer-coated CPT nanoparticles, as described in Example 2, in accordance with an aspect of the invention;

[0016] FIG. 7 is the FT-IR spectra showing the degradation of functional groups of the PCL polymeric coating on PCL polymer-coated CPT nanoparticles as described in Example 3, according to an aspect of the invention;

[0017] FIG. 8A is a graph showing the percent release of the CPT therapeutic agent from PCL polymer-coated CPT nanoparticles at a pH of 6.0 as described in Example 4, according to an aspect of the invention;

[0018] FIG. 8B is a graph showing the percent release of the CPT therapeutic agent from PCL polymer-coated CPT nanoparticles at a pH of 6.5 as described in Example 4, according to an aspect of the invention;

[0019] FIG. 8C is a graph showing the percent release of the CPT therapeutic agent from PCL polymer-coated CPT nanoparticles at a pH of 7.4 as described in Example 4, according to an aspect of the invention;

[0020] FIG. 9 is a plot of the

$$\log\left(\frac{M_t}{M_\infty}\right)$$

vs. $\log t$ to describe the drug release behavior of the PCL polymer-coated CPT nanoparticles as described in Example 4, according to an aspect of the invention;

[0021] FIG. 10 is a growth inhibition curve of HER-2 positive tumor cells in response to various concentrations of PCL polymer-coated CPT nanoparticles conjugated with a TTZ antibody or with BSA as described in Example 5, in accordance with an aspect of the invention;

[0022] FIG. 11 is a growth inhibition curve of HER-2 negative tumor cells in response to various concentrations of PCL polymer-coated CPT nanoparticles conjugated with a TTZ antibody or with BSA as described in Example 5, in accordance with an aspect of the invention; and

[0023] FIG. 12 is a schematic depiction of a FRET-based system for the detection of cancer DNA, according to an aspect of the invention.

DETAILED DESCRIPTION

[0024] In various aspects, polymer-coated therapeutic nanoparticles are disclosed. In certain aspects, the polymer-coated therapeutic nanoparticles can include one or more therapeutic agents at least partly covered with an outer polymeric coating. In various aspects, one or more targeting molecules can be associated with the outer polymeric coating in order to target the therapeutic nanoparticle to a particular site, such as a tumor or another particular type of cell.

[0025] Formulating active therapeutic agents for targeted delivery and effective drug release at the target site remains one of the top challenges for effective treatments of various illnesses or diseases. In certain scenarios, an active agent in a therapeutic formulation may undergo modification when administered and be eliminated prior to the active agent reaching a target site, e.g., a tumor or organ. One exemplary active agent where such problems can occur is the anti-cancer chemotherapy drug camptothecin (CPT). CPT has a lactone ring that gets converted to a carboxylate at a physiological pH of 7.4. Once the lactone ring in CPT is converted to a carboxylate, its affinity to human serum albumin (HAS) is increased and preferably becomes bound to HAS, which promotes the elimination of CPT from the body, prior to it having a chance to reach a target tumor site, thereby reducing the efficacy and bioavailability of the active ingredient therapeutic agent (CPT). Because of this rapid elimination, it becomes necessary to increase the therapeutic agent, which in turn increases the toxicity of this chemotherapy.

[0026] Certain current strategies or methods have been utilized to prevent the conversion and/or degradation of an active agent, such as CPT. However, some of these CPT formulations have been known to cause hepatic toxicity and renal failure, and/or tend to aggregate, which reduces their bioavailability.

[0027] The polymer-coated therapeutic nanoparticles described herein address one or more of the problems mentioned above. In certain aspects, the polymer-coated therapeutic nanoparticles can effectively protect an active therapeutic agent while that agent is specifically delivered to a target site. In such aspects, the polymer-coated therapeutic nanoparticles can include an outer polymeric coating including one or more biodegradable or bio-responsive polymers that can prevent the premature degradation and/or modification of the therapeutic active agent once administered to a patient. Further, in such aspects, one or more targeting molecules can be associated with the outer polymeric coating to target the therapeutic active agent to a particular target site, such as a tumor. In certain aspects, the outer polymeric coating can maintain at least partially intact under general physiological conditions (e.g., pH 7.4), and may at least partially degrade in the local physiological conditions associated with a tumor (e.g., a lower pH of about 6.0 to about 6.5). In such aspects, the polymer-coated therapeutic nano-

particles may stay coated and protected from degradation until it reaches its target site, such as tumor, at which time the outer polymeric coating can be degraded thereby releasing the inner therapeutic active agent. Further, in various aspects, the polymer-coated therapeutic nanoparticle may be rod-shaped to allow for increased cellular uptake and/or reduced phagocytosis, both of which may increase the effectiveness of the therapeutic agent.

[0028] In certain aspects, an elongated rod-shaped design of the polymer-coated therapeutic nanoparticles allows for long circulation time in the body, and multivalent interactions with target cells, such as tumor cells, increasing the probability of receptor-ligand interactions. In such aspects, due to the fluid dynamics induced by the unique rod shape, the nanoparticles can flow along the edges of blood vessels. By flowing along the sides of blood vessels, nanoparticles may reach the target cells, e.g., tumor or cancer cells, due to the gaps in the endothelial cell wall between the tumorous tissue and the blood vessels.

[0029] Furthermore, as discussed above, the microenvironment of tumorous tissue can be slightly more acidic with a pH of about 6-6.5, as compared to the pH of blood, which has a pH of about 7.4. This discrepancy in pH may be advantageously used in accordance with aspects of the present invention where the outer polymer coating may be selected to be resistant to degradation at pH 7.4, but quickly degrades at the more acidic pH of the tumorous tissue, thereby effectively releasing the therapeutic agent at the desired site of action. Thus, in certain aspects, the polymer-coated therapeutic nanoparticles can be customized taking into consideration the target microenvironment to increase the efficacy of the therapeutic agent by several fold, while at the same time reducing the side effects of the therapeutic agent because effective concentrations of the therapeutic agent can be delivered to target sites at lower doses.

[0030] FIG. 1 is a schematic view of one aspect of a polymer-coated therapeutic nanoparticle 100. The polymer-coated therapeutic nanoparticle 100 of FIG. 1 includes an inner core 102, an outer polymeric coating 104, and one or more targeting molecules 106. The inner core 102 can include one or more therapeutic agents. In certain aspects, the therapeutic agent can include any pharmaceutical. In one or more aspects, the therapeutic agent can include an anti-cancer agent, such as CPT.

[0031] In certain aspects, the inner core 102 can include at least about 20 wt. %, at least about 40 wt. %, at least about 50 wt. %, at least about 60 wt. %, at least about 70 wt. %, at least about 80 wt. %, at least about 90 wt. %, at least about 95 wt. %, at least about 99 wt. %, or about 100 wt. % therapeutic agent relative to the weight of the inner core 102. In certain aspects, the therapeutic agent may be present in high concentrations in the inner core 102 at least partly because the outer polymeric coating 104 can encapsulate and protect the inner core 102 comprising the therapeutic agent, thereby minimizing or eliminating the need for excipients in the formulation of the therapeutic agent, such as fillers and stabilizers, depending on the specific chemistry of the therapeutic agent.

[0032] In aspects where the inner core 102 include less than about 100 wt. % therapeutic agent, the remainder can include one or more pharmaceutically acceptable excipients. In various aspects, one or more pharmaceutically acceptable excipients can be present in the inner core 102 in an amount of at least about 0.01 wt. %, at least about 0.1 wt. %, at least

about 1 wt. %, at least about 5 wt. %, or at least about 10 wt. %, and/or less than about 50 wt. %, less than about 40 wt. %, less than about 30 wt. %, less than about 20 wt. %, or less than about 15 wt. % relative to the weight of the inner core **102**. It is appreciated that pharmaceutically acceptable excipients are commercially available and can be chosen by one skilled in art for a specific purpose. Examples of such excipients can be found, for example, in the Handbook of Pharmaceutical Excipients, 7th ed., 2012, Pharmaceutical Press, incorporated herein by reference.

[0033] In various aspects, the inner core **102** can be rod-shaped. As used herein, a rod-shaped inner core refers to the inner core having an elongated cylindrical (where the length *l* is greater than the diameter *d*) or rectangular shape (where the length *l* is greater than the width *w*). In certain aspects, the entire polymer-coated therapeutic nanoparticle **100** can be rod-shaped.

[0034] In certain aspects, the inner core **102** can have a length or maximum dimension of about 450 nm or less, about 400 nm or less, about 350 nm or less, about 300 nm or less, about 250 nm or less, about 200 nm or less, or between about 150 nm and about 200 nm, between about 100 nm and about 400 nm, between about 150 and about 300 nm, between about 50 nm and about 300 nm, between about 10 nm and about 400 nm, or between about 10 nm and about 200 nm. As used herein, maximum dimension of the inner core **102** refers to the largest dimension of the inner core **102**. For example, for a rod-shaped inner core, the maximum dimension refers to the largest of the length and diameter if the inner core is an elongated cylindrical shape, or the largest of the length, width, and depth of the rod-shaped inner core if the inner core is rectangular shaped.

[0035] In one or more aspects, the outer polymeric coating **104** can include one or more polymers. In various aspects, the polymers used in the outer polymeric coating **104** should be non-toxic so that they can be administered to a patient. In certain aspects, the polymer can be a biodegradable and/or bio-responsive polymer. As used herein, a bio-responsive polymer refers to a polymer that is capable of at least partly being chemically broken down when exposed to a particular physiological environment. For example, as discussed in detail below, poly(ϵ -caprolactone) (PCL) can be at least partly chemically degraded at a pH of about 6, but not at all (or less so) at pH 7.4. In this example, PCL would not be substantially degraded in the blood (approximately a pH of 7.4) but would be at least partly degraded at a lower pH of about 6 (approximately the pH associated with a tumor microenvironment). In certain aspects, a biodegradable polymer can be a polymer that is capable of at least being partially chemically broken down in a particular biological environment, such as via bacteria or the like.

[0036] In certain aspects, the outer polymeric coating **104** can include poly(ϵ -caprolactone) (PCL), polylactic acid (PLA), Poly(lactic-co-glycolic acid) (PLGA), hyaluronic acid (HA), poly(acrylic acid) (PAA), poloxamers, polyethylene oxide (PEO), polyethylene glycol (PEG), polyflutamic acid, or a mixture thereof. It is appreciated that one skilled in the art would understand that other polymers or other materials could be used for the outer polymeric coating **104** as long as such materials are non-toxic in the sense that they can be administered to a patient as a coating for at least one therapeutic agent.

[0037] As can be seen in FIG. 1, the outer polymeric coating **104** entirely encapsulates the inner core **102**. In

alternative aspects, the outer polymeric coating **104** may partly encapsulate the inner core **102**.

[0038] In certain aspects, the outer polymeric coating **104** can have a maximum thickness *t* of about 150 nm or less, about 100 nm or less, about 80 nm or less, about 50 nm or less, about 30 nm or less, about 10 nm or less, or between 1 nm and 100 nm, between 1 and 50 nm, or between 5 and 70 nm.

[0039] As can be seen in FIG. 1, the outer polymeric coating **104** is a substantially even coating, meaning that it has substantially the same thickness throughout the coating. In certain aspects not depicted in the figures, the outer polymeric coating may vary in thickness; yet, the maximum thickness of the coating in this instance can be within the maximum thickness parameters immediately described above.

[0040] As discussed above, in various aspects, one or more targeting molecules **106** may be associated with the outer polymeric coating **104**. In such aspects, the targeting molecules **106** can facilitate the targeted delivery of the therapeutic agent to a specific target site, such as a tumor. In certain aspects, the targeting molecule can include one or more antibodies or fragments of antibodies, or other polypeptides. In certain aspects, the fragments of one or more antibodies include the antigen binding region commonly known as the fragment antigen binding (Fab) fragment. In such aspects, the Fab fragment may be formed by enzymatic digestion of a full length antibody. In alternative aspects, the targeting molecule can include molecules other than proteins, such as synthetic or natural receptor ligands.

[0041] In certain aspects, the antibodies, polypeptides, or other targeting molecules may be selected to be specific to the type of cells to be treated by, for example, matching the antibodies or polypeptides to receptors overexpressed in cancerous tissues such as human epidermal growth factor receptor 2 (HER-2) in breast cancer, or G-protein-coupled receptors (GPCRs), which has been linked to cancers such as melanoma, lymphoma, lung cancer, gastric cancer, etc. Thus, in such aspects, the targeting molecule will work to increase the concentration of the polymer-coated therapeutic nanoparticle at the tumor site and release the therapeutic agent in the inner core at the tumor site due to the degradation of the outer polymeric coating in the tumorous tissue microenvironment, e.g., due to the lower pH of this microenvironment.

[0042] In certain aspects, the targeting molecule may be covalently attached to the outer polymeric coating. For example in such aspects, an ester functional group in a portion of a polymer in the outer polymeric coating can react with an available amine functional group of a polypeptide or antibody target molecule to form an amide bond thereby covalently attaching the target molecule to the outer polymeric coating and to the polymer-coated therapeutic nanoparticles. FIG. 2 provides one example of a target molecule conjugated to the outer polymeric coating via an amide bond. In the example of FIG. 2, an ester group of the PCL polymer, e.g., in the outer polymeric coating, can react with an amine group on the Herceptin (Trastuzumab) monoclonal antibody to form an amide bond covalently attaching the Herceptin antibody to the outer polymeric coating. In the example of FIG. 2, the ester group of the polymer and the amine group of the targeting molecule are not sterically hindered, which allows for this covalent attachment while

avoiding any preliminary modifications of the antibody or polypeptide, which may reduce the activity of the antibody or polypeptide.

[0043] While an ester functional group of an exemplary polymer is used in the above example to illustrate the covalent attachment of the targeting molecule to the outer polymeric coating, it is appreciated that other functional groups (such as a carboxylic acid functional group) in a polymer used in the outer polymeric coating can be used to provide for a covalent attachment to a targeting molecule. Further, it is appreciated that one skilled in the art would be able to modify a portion of a polymer in the outer polymeric coating in order to provide for a covalent attachment between the polymer in the outer polymeric coating and a targeting molecule, for example, by converting a portion of the polymer to a carboxylic acid or ester functional group.

[0044] As discussed above, in certain aspects a method of producing the polymer-coated therapeutic nanoparticles is provided. In certain aspects, a solvent diffusion method can be utilized to form the polymer-coated therapeutic nanoparticles. In the solvent diffusion method, a therapeutic agent in an organic solvent, such as dimethyl sulfoxide (DMSO), and a polymer for the outer polymeric coating in an organic solvent, such as toluene, are separately injected, e.g., via a syringe pump, into an aqueous solution, e.g., water. The therapeutic agent solution and the polymer solution can be injected into the aqueous solution simultaneously or sequentially. In one aspect, the therapeutic agent solution and the polymer solution are injected into the aqueous solution simultaneously. Without being bound by any particular theories, it is believed that when the therapeutic agent solution is injected into the aqueous solution, an inner core nanoparticle of the therapeutic agent is formed because of the phase separation from the DMSO oil phase into the water (or aqueous solution) under mild stirring. Further, without being bound by any particular theory, it is believed that at the same time that the inner core is formed, a continuous or semi-continuous polymer film coats the inner core by virtue of van der Waals attractive forces between the inner core particle surface and the polymer under low shear stress, and it is also believed that the combination of adhesive and shear forces spread the polymer thinly over each inner core particle. The dispersion may be stirred continuously for an extended period of time to remove any residual organic solvent by evaporation. After the residual organic solvent is removed by evaporation, the polymer-containing therapeutic nanoparticles may then be separated from the aqueous phase by centrifugation, repeating this step as necessary with added water, for washing the nanoparticles from any residual organic solvents. Then, the polymer-containing therapeutic nanoparticles may be lyophilized, weighed, and stored at a temperature of about 4° C. It is appreciated that one skilled in the art understands that the concentration of polymer(s) in the organic solvent, the concentration of the therapeutic agent in an organic solvent, the injection rate of the polymer solution and/or the therapeutic agent solution into the aqueous solution, and/or the particular components of the aqueous solution can be modified to achieve specific sized and shaped nanoparticles.

[0045] In certain aspects, the concentration of polymer in the organic solvent or the therapeutic agent in the organic solvent can range from about 0.1 mg/mL to about 1000 mg/mL, or from about 1 mg/mL to about 100, or can be at least about 0.1 mg/mL, or at least about 1 mg/mL. In certain

aspects, the concentration of polymer in an organic solvent can be about 1 mg/mL and the concentration of the therapeutic agent in an organic solvent can be about 10 mg/mL. In one or more aspects, the flow rate or injection rate of the organic solvent comprising one or more polymers into the aqueous phase can range from about 0-1000 $\mu\text{L}/\text{sec}$. Further, in certain aspects, the flow rate or injection rate of the organic solvent comprising the therapeutic agent into the aqueous phase can range from about 0-1000 $\mu\text{L}/\text{sec}$.

[0046] FIG. 3 depicts an exemplary system **300** that can be utilized to synthesize polymer coated therapeutic nanoparticles using a solvent diffusion method. The system **300** can include a syringe pump **302** for injecting the polymer-containing solution via line **304** and the therapeutic agent-containing solution via line **306** into an aqueous solution **310** housed in a vessel **308**. A homogenizer **312** can also be positioned inside the vessel **308**. It is appreciated that the components of this system **300** are commercially available and known to one skilled in the art.

[0047] In various aspects, the solvent diffusion method described above can result in the formation of a plurality of polymer-coated therapeutic nanoparticles. In certain aspects, the polymer-coated therapeutic nanoparticles can have a substantially uniform size. In alternative aspects, the polymer-coated therapeutic nanoparticles can have different sizes. In one or more aspects, the polymer-coated therapeutic nanoparticles can have a polydispersity index value of about 0.05, 0.1, 0.2, 0.3, or 0.4.

[0048] In certain aspects, methods for treating a patient are provided. In such aspects, these methods can include administering a therapeutically effective amount of polymer-coated therapeutic nanoparticles. In certain aspects, a therapeutically effective amount can be an amount sufficient to provide a biologically beneficial effect to the subject such as by producing a beneficial change in a disease state or inhibiting the progression of a disease, such as preventing or reducing tumor growth or cancer cell growth.

[0049] In certain aspects, the polymer-coated therapeutic nanoparticles can be administered to a subject using any conventional routes of administration known to one skilled in the art. A non-limiting list of such routes includes administration intravenously, subcutaneously, by pill, topically, and local administration.

[0050] In one or more aspects, prior to administration, the polymer-coated therapeutic nanoparticles may be mixed with one or more inactive ingredients, such as solvents, diluents, additives, pharmaceutically acceptable excipients, enhancers, pharmaceutically acceptable carriers, and combinations thereof. It is appreciated that such inactive ingredients may be chosen by one skilled in the art for a particular route of administration and other common considerations. As such, such administration formulations and components will not be further described herein.

EXAMPLES

Polymer-Coated Therapeutic Nanoparticles

[0051] The concepts discussed herein will be further described in the following examples, which do not limit the scope of the various aspects described in the claims.

[0052] Each experiment in the below examples that included quantified measurements was carried out in at least

three independent experiments with triplicate measurements. Data were summarized using means and standard deviations.

Example 1

Synthesis of PCL Polymer-Coated Camptothecin (CPT) Therapeutic Nanoparticles

[0053] All reagents were purchased from Sigma-Aldrich unless otherwise specified. A thin layer of continuous PCL polymer (14,000 Da) film was deposited on inner core CPT nanoparticles using the solvent diffusion method. Specifically, 1 mL each of 10 mg/mL of CPT in DMSO and 1 mg/mL of PCL polymer in toluene were added to 20 ml of reverse osmosis (RO) water using a syringe pump, such as the syringe pump **302** discussed above with reference to FIG. **3**. Residual toluene was removed by stirring (300 rpm) the CPT-PCL nanoparticle suspension overnight at room temperature ($\sim 22^\circ\text{C}$). DMSO was removed by centrifugation at 3,000 rcf, followed by five times washing using RO water. PCL-coated CPT (CPT-PCL) nanoparticles were freeze-dried, weighed and stored at 4°C . CPT concentrations were measured, and quantified by reading absorbance at 366 nm using a plate reader (BioTek Synergy), and the CPT calibration curve shown in FIG. **4**. The theoretical content of the PCL polymer weight in the CPT-PCL nanoparticles was calculated based on the weight of freeze-dried particles and CPT amount. The dry w:w ratio of CPT:PCL was 0.03.

Example 2

Characterization of CPT-PCL Nanoparticles

[0054] The morphology and size of CPT-PCL nanoparticles produced in Example 1 were examined under transmission electron microscope (TEM) (Tecnai F20) at an accelerating voltage of 120 kV. A drop of 10 μl CPT-PCL nanoparticle solution in water was air-dried on carbon-coated copper grids (Tedpella). The CPT-PCL nanoparticle diameter, CPT-PCL nanoparticle length, and thickness of the PCL outer polymeric coating were measured using ImageJ (version 1.45S, NIH, USA) for at least 20 CPT-PCL nanoparticles. FIGS. **5A** and **5B** show representative TEM images. As can be seen in FIGS. **5A** and **5B** the polymer-coated therapeutic nanoparticles have a rod-shape. These rod-shaped CPT-PCL nanoparticles had a length or maximum dimension of $500.9\text{ nm}\pm 91.3\text{ nm}$ and a width or diameter of $122.7\text{ nm}\pm 10.1\text{ nm}$. Further, based on these TEM images, the PCL coating thickness was determined to be $10.3\pm 1.4\text{ nm}$. This is a soft coating technique that does not require high mechanical agitation, sonication or vibration, thus preventing any structural damage of therapeutic agents in the inner core.

[0055] The surface charges of the CPT-PCL nanoparticles in PBS were determined by dynamic light scattering (DLS) using a NanoSeries Zetasizer ZS 90 (Malvern) and the backscattering detection at 90° . The zeta potential was measured for the CPT-PCL nanoparticles for 15 runs. For comparison, the zeta potential was also measured for CPT nanoparticles lacking the PCL polymer coating. Data was analyzed using means and standard deviations of three concentrations. The results are shown in FIGS. **6A** and **6B** for the CPT nanoparticles alone in and the CPT-PCL nanoparticles, respectively. Both samples were in phosphate

buffered saline (PBS). The zeta potential of the CPT nanoparticles alone was $-26.8\pm 7.71\text{ mV}$, while the zeta potential of the CPT-PCL nanoparticles was $-15.5\pm 3\text{ mV}$. An increase in zeta potential for the CPT-PCL nanoparticles indicates the deposition of the PCL polymer on the surface of CPT inner core particles.

Example 3

Degradation of the PCL Coating on the CPT-PCL Nanoparticles

[0056] The degradation of the PCL coating of the CPT-PCL nanoparticles made in Example 1 was analyzed by Fourier transform infrared spectroscopy "FT-IR spectroscopy." The disappearance of ester groups in the PCL backbone, and appearance of carboxyl and hydroxyl groups were studied using FT-IR spectra. CPT-PCL nanoparticles were incubated for 72 hours at 37°C in PBS at pH 6 (which mimics the slightly acidic cancer microenvironment). Samples were freeze-dried to sublimate any water, and ground at a 1:100 weight ratio with FT-IR grade potassium bromide (KBr; Alpha Aesar). Hydrolytic degradation was monitored by comparing the intensity of ester, alcohol and carboxyl bands at $t=0$ and 72 h for the same amount of PCL in NRs. The FT-IR absorbance spectra were obtained for 32 scans over the range of $4000\text{--}400\text{ cm}^{-1}$ using a Thermo Nicolet Nexus 470 FT-IR spectrometer. Background noises were subtracted from the spectra. All spectra were analyzed using EZ OMNIC E.S.P v.5.1 software. FIG. **7** shows the FT-IP spectra.

[0057] The presence of a strong band at 1728 cm^{-1} is due to the presence of an ester carbonyl group that corresponds to the —CO stretching in the PCL polymer coating before degradation (dotted line). The band intensity decreased at 1728 cm^{-1} after 72 h due to hydrolytic cleavage of ester bonds at pH 6 (solid line). The peak at 1288 cm^{-1} represents C—C and C=O stretching in the PCL polymer backbone. The peaks at 2860 and 2931 cm^{-1} correspond to the characteristic absorption of the C—H stretching bonds of $\epsilon\text{-CL}$. The appearance of two peaks at 1652 cm^{-1} and 3440 cm^{-1} indicate the presence of carboxyl (—COOH) and hydroxyl (—OH) groups, respectively. These peaks represent the hydrolysis of ester bonds, forming a carboxylic acid group and an organic alcohol. The —OH group attributes to the formation of alcohol group as well as the OH group of lactone ring of CPT, indicating the retention of the active ring of CPT.

Example 4

Quantification of CPT Drug Release from the CPT-PCL Nanoparticles

[0058] CPT drug release was monitored by exposing CPT-PCL nanoparticles to phosphate buffered saline (PBS) at pH 6 or pH 6.5 (to mimic the cancer microenvironment), or at pH 7.4 (to mimic the pH of blood) and at 37°C without stirring. 500 μl of the PBS buffer were sampled at different time intervals of $t=0, 0.5, 2, 4, 8, 24, 36$ and 72 h. CPT drug concentrations that were released to the buffer were measured using absorbance at 366 nm and a CPT standard curve (shown in FIG. **4**). FIGS. **8A**, **8B**, and **8C** show the % CPT released over time at a pH of 6.0, 6.5, and 7.4, respectively. As can be seen in FIGS. **8A**, **8B**, and **8C** the degradation of the PCL coating as evidenced by the CPT release is signifi-

cantly faster from the 2 hour to 24 hour time period for the CPT-PCL nanoparticles in PBS solutions at a pH of 6.0 (FIG. 8A) and 6.5 (FIG. 8B) compared to the CPT release over the same time period (2-24 hours) for the CPT-PCL nanoparticles in PBS solutions at a pH of 7.4 (FIG. 8C). These results show that the CPT-PCL nanoparticles release more CPT in a tumor microenvironment (e.g., pH 6.0 to pH 6.5) than in the blood (e.g., pH 7.4).

[0059] Looking more closely at the data in FIG. 8A, a slow release was observed with 8.2% CPT release in the first 0.5 h following 32.6% release after 8 h, and 51.5% after 72 h. CPT was released from the PCL-coated nanoparticles by

stirring to mix, and incubated the mixture at room temperature (~25° C.). Any unreacted reagents were separated using 100 kDa membrane filters (EMD Millipore Amicon Ultra-0.5). The supernatants were collected by centrifugation at 1,000 rcf, and analyzed by the BCA protein assay (Pierce Thermo Scientific). Bovine serum albumin (BSA) was used to prepare HER-2 non-targeted CPT-PCL NRs as HER-2 negative controls (TTZ binds to HER-2). TTZ covalent binding would help deliver the CPT-PCL nanoparticles to breast cancer cells. Using the BCA protein assay, it is calculated that the weight ratio of CPT:PCL:TTZ is 1:29:3.5 (Table 1 below). The ratio of CPT:PCL:BSA was almost the same as 1:29:2.1 (Table 1).

TABLE 1

Weight ratios of CPT, PCL, and TTZ							
Amount of CPT in CPT-PCL-TTZ nanoparticles, μg	TTZ in CPT-PCL-TTZ nanoparticles, μg	PCL in CPT-PCL-TTZ nanoparticles, μg	CPT:PCL:TTZ W:W Ratio	CPT in CPT-PCL-BSA nanoparticles, μg	BSA in CPT-PCL-BSA nanoparticles, μg	PCL in CPT-PCL-BSA nanoparticles, μg	CPT:PCL:BSA W:W Ratio
715.44 \pm 186.88	2512.65 \pm 444.87	20824.09 \pm 5439.37	1:29:3.5	848.38 \pm 277.55	1755.78 \pm 772.16	24693.05 \pm 8078.55	1:29:2.1

hydrolytic disruption of the PCL coating and the drug's diffusion. The CPT drug release data were fitted to the following well-known power law equation (2) that describes the drug release behavior from polymeric systems:

$$\frac{M_t}{M_\infty} = kt^n \quad (2)$$

where

$$\frac{M_t}{M_\infty}$$

is the fraction of drug released at time t, k is the kinetic constant, and n is the diffusion exponent for drug release. By plotting

$$\log\left(\frac{M_t}{M_\infty}\right)$$

vs. log t (as shown in FIG. 9), n was calculated as 0.4 for CPT drug release, indicating a Fickian drug diffusion.

Example 5

Conjugation of an Antibody on the Surface of CPT-PCL Nanoparticles

[0060] Trastuzumab (TTZ) antibody (Genentech) was conjugated to the surface of CPT-PCL nanoparticles by coupling primary amines of TTZ with ester groups of PCL forming amide bonds. Specifically, a 10 mg/ml TTZ solution was prepared in PBS at pH 7.4. 10 mg of CPT-PCL nanoparticles were added to 1 ml of the TTZ solution,

Example 6

Breast Cancer Cell Growth by CPT-PCL Nanoparticles Conjugated with TTZ Antibody

[0061] The effectiveness of combination treatments using PCL-CPT-TTZ nanoparticles were evaluated in HER-2 positive BT-474 breast cancer cells (ATCC) and HER-2 negative cell line MDA-MB-231 (ATCC). The cells were cultured in Hybri-Care (ATCC), and RPMI 1640 (Life Technologies), respectively supplemented with 10% FBS (Corning) and 1% (100 units/ml) Penicillin-Streptomycin (Gibco) at 37° C. and 5% CO₂. HUVEC cells (Invitrogen) were used as a normal cell control that was cultured in Medium 200 (Invitrogen) with Low Serum Growth Supplement (LSGS) kit (Invitrogen). Cells were plated in 96-well tissue culture plates (Corning) at a density of 10,000 cells/well in 200 μl respective medium. After 18 hours of growth, 10 μl of nanoparticles made in Example 5 were added to the medium. The final concentrations of CPT were 0.1, 0.2, 0.5, 1, 2, 5 and 10 $\mu\text{g}/\text{ml}$. The corresponding PCL concentrations were 2.9, 5.8, 14.6, 29.1, 58.2, 145.5, and 291.1 $\mu\text{g}/\text{ml}$, respectively, and TTZ concentrations were 0.4, 0.8, 1.9, 3.8, 7.5, 18.8, and 37.7 $\mu\text{g}/\text{ml}$, respectively. CPT-PCL-BSA nanoparticles made in Example 5 were used as a HER-2 non-specific control. Cells were also treated with the same concentrations of PCL solutions to determine its cytotoxic effects. Cells treated with 10 μl of PBS were used as positive controls. 3 hours later, the medium was replaced with fresh medium. After 72 hours, the plates were centrifuged at 100 rcf for 15 min. The supernatants were discarded. Live cells were stained with 2 μM calcein AM (Life technologies) in PBS by incubating at room temperature for 30 min. The fluorescence intensity (F.I.) of calcein AM was measured using 485/528 excitation/emission filters using the plate reader (BioTek Synergy 2). The percentage inhibition in cell growth was calculated using the following equation (2):

% inhibition in cell growth = (2)

$$\frac{F.I. \text{ of PBS treated cells} - F.I. \text{ of samples}}{F.I. \text{ of PBS treated cells}} \times 100$$

[0062] The therapeutic activity of CPT-PCL-TTZ nanoparticles was evaluated in HER-2 positive BT-474 (FIG. 10) and HER-2 negative MDA-MB-231 cells (FIG. 11) at varying concentrations. These are the previously reported dosage amounts of CPT in human breast cancer cells. The NRs inhibited the growth of HER-2 positive BT-474 cells in a dose dependent manner. The combination of CPT and TTZ using CPT-PCL-TTZ nanoparticles inhibited up to 61.6% BT-474 cell growth at 10 $\mu\text{g/ml}$. At this concentration, CPT-PCL-TTZ nanoparticles inhibited the cell growth 1.5 fold more than CPT-PCL-BSA nanoparticles. The difference in growth inhibition between CPT-PCL-TTZ nanoparticles and CPT-PCL-BSA nanoparticles indicates the antibody dependent growth inhibition effects of TTZ on HER-2 positive BT-474 cells. Interestingly, HER-2 negative MDA-MB-231 cell line was also sensitive to the nanoparticles. No difference between CPT-PCL-BSA nanoparticles and CPT-PCL-TTZ nanoparticles was found in HER-2 negative MDA-MB-231 cells, indicating non-specific CPT-evoked growth inhibition.

Engineering Glass Nanofibers and Fluorescent Polymers for Early Cancer Diagnosis

[0063] In certain aspects, systems and methods are disclosed that are directed to the early diagnosis of cancer using fluorescent polymers or fluorescent glass nanofibers.

[0064] Finding early relevant cancer in people with no symptoms, as opposed to diagnosing the disease in its advanced stage, can be an important part of diagnosing and treating cancer patients. We have aimed to design an imaging agent using a conjugate of fluorescent glass nanofibers (such as those that are commercially available, e.g., from the MO-SCI Corporation) or fluorescent polymers and DNA staining organic dyes for detecting any alterations in normal DNA into a tumor DNA. The common characteristics of DNA deregulation are going to be stored in a computational database to generate information on suspected DNA allowing intervention of cancer prior to its progression and implementation into clinical applications as a non-invasive method. FIG. 11 illustrates a flow 1100 of a hypothesis on FRET-based detection of cancer DNA using a conventional nucleic acid stain (NAS) as FRET acceptor and GNF as FRET donor. The GNF-NAS conjugates will display photostable fluorescence emission to image the chromatin of the nucleus to detect any abnormalities in DNA. Diagnosing and monitoring cancers have been developed extensively during the last two decades to detect cancer cells early. However, most of the approaches diagnose the disease at the advanced stage when the biomarkers are overexpressed on cancer cells, or circulated in the patient's blood. In addition, the existing methods require cumbersome and time consuming experiments to isolate, process and analyze the samples.

[0065] As discussed further herein, a fluorescence resonance energy transfer (FRET) based nuclear sensor for the early detection of cancer cells has been developed by imaging and analyzing the structural alterations e.g., morphology, shape, size and nuclear matrix of the cell nuclei more easily. A comprehensive computational database on

the pattern of DNA malfunction is going to be used to track any symptoms of a healthy versus risky nucleus at an early stage.

[0066] For background purposes, early detection of cancer can decrease the mortality rate of some major cancers. There are a variety of screening tests such as body fluid (blood, urine, saliva etc.) biomarker tests, circulating tumor cell identification, cell free nucleic acid (NA) detection and breathing tests among others for early cancer detection. Nanoparticles (NPs) have also been used for the detection of biomarkers. However, current systems suffer from false positive or negative results, and are limited only for aggressive cancers and not applicable to detect cancer at the early stage. Alterations in NAs are common characteristics of tumor progression, and can be used for diagnosis. However, no such NPs have been developed to characterize the nuclei in cancer phenotypes. Here, we propose to synthesize a FRET-based conjugate using fluorescent glass nanofibers (such as those that are commercially available, e.g., from the MO-SCI Corporation) or fluorescent polymers as donors, and NA staining organic dyes such as propidium iodide (PI) or SYTO stain as acceptors.

[0067] Recently, fluorescent glass nanofibers (GNFs) (www.mo-sci.com/identisphere) and fluorescent polymers have emerged as biomarkers. The spectral overlap of emission of GNFs with the absorption wavelength of nuclear dye acceptor gives a favorable condition for FRET from GNFs to nucleic acid stain (NAS)s (see e.g., FIG. 12). When the FRET donor and acceptor molecules are brought in close proximity (~1-10 nm) to each other, in this project the GNF and NAS, respectively, energy transfers from GNF (donor) to NAS (acceptor) upon excitation at GNF's excitation wavelength resulting in fluorescence emission of NASs at longer wavelengths.

[0068] Preliminary studies have been performed that demonstrate the feasibility of the proposed studies. Some of our findings were as follows. The nuclei of prostate cancer cells were imaged under confocal fluorescence microscopy showing irregular shaped heterochromatin with dispersed aggregates. The nuclear membrane as stained by the lamin antibody showed folded, discrete and inhomogeneous nuclear membrane. Detailed structures of the cancer cell nucleus were required to describe these abnormalities.

[0069] A novel, sensitive NA staining probe has been developed by conjugating GNFs with organic NASs, as shown in FIG. 11. Additionally, new analytical methods have been developed to readout descriptive statistics of nuclear size, shape, chromatin distribution and abnormal textures of chromatin. It is noted that while fluorescent glass nanofibers are described herein, fluorescent polymers, such as those that are commercially available, may also be used in conjunction with the methods and systems herein.

Example A

Synthesis of GNF and NAS Conjugates

[0070] GNFs will be conjugated with DNA binding molecules using activated carboxyl groups on GNFs and amines on NAS by EDC/NHS chemistry. The emission of GNFs at the excitation range of NASs will serve as an appropriate FRET donor, and thus can create stable fluorescent signals of NAS. Light spectroscopy and fluorescence will be quantified for both GNFs and NASs by measuring their absorbance, excitation and emission spectra using a confocal

microscope and single cell imaging system. FRET efficiency will be measured using the fluorescence intensity of GNF in presence and absence of NAS. The size and shape of the particles will be determined using dynamic light scatter and SEM.

Example B

Fluorescence Imaging and Quantification Using ImageJ Analysis

[0071] The nuclear architectures of cancer cells are significantly different than normal cells. The nuclear changes in cancer cells include irregular shape, abnormal folds inside nuclear membrane, coarse heterochromatin aggregates and abnormal nucleoli. Imaging cellular nucleus using a fluorescent GNF probe, therefore, is highly desirable to speculate on the possible correlations between nuclear changes and cancer progression. Fluorescence confocal microscopy, single cell imaging and image analysis systems will be used to analyze GNF conjugated NAS. Various cancers including breast, prostate, colon and lung cancers and normal cell lines will be incubated with particles to image the cell nuclei. ImageJ software will be used to quantitatively measure nuclear architecture such as size, shape and number of chromosomes. The average nuclear size will be calculated for ~50 nuclei for each sample of normal versus cancer cells to identify the development of cancer. A percentage deviation of 10-20% will be considered as a cancer threshold. A database will be developed defining the area, volume, nuclear boundary, and chromatin texture features from the statistical analysis of the fluorescence levels of the microscopic images. In vivo fluorescence imaging will be accomplished in the future after establishing the in vitro model. This method will speed up the early diagnosis of cancer leading to a greater chance of survival for any patients with defective chromosomal diseases at a fraction of the cost of commonly used imaging studies.

[0072] From the foregoing, it will be seen that this invention is one well adapted to attain all the ends and objects hereinabove set forth together with other advantages which are inherent to the systems and methods.

[0073] It will be understood that certain features and subcombinations are of utility and may be employed without reference to other features and subcombinations. This is contemplated by and is within the scope of the claims.

[0074] Since many possible aspects may be made of the invention without departing from the scope thereof, it is to be understood that all matter herein set forth or shown in the accompanying drawings is to be interpreted as illustrative and not in a limiting sense.

What is claimed is:

1. A polymer-coated therapeutic nanoparticle, comprising:

an inner core comprising at least one therapeutic agent, wherein the inner core has a maximum dimension of 300 nm or less; and

an outer polymeric coating that coats at least a portion of the inner core, wherein the outer polymeric coating has a thickness of 1 nm to 100 nm.

2. The polymer-coated therapeutic nanoparticle of claim 1, further comprising a targeting molecule associated with the outer polymeric coating.

3. The polymer-coated therapeutic nanoparticle of claim 2, wherein the targeting molecule is covalently bonded to at least a portion of the outer polymeric coating.

4. The polymer-coated therapeutic nanoparticle of claim 2, wherein the targeting molecule comprises an antibody.

5. The polymer-coated therapeutic nanoparticle of claim 2, wherein the targeting molecule comprises a polypeptide.

6. The polymer-coated therapeutic nanoparticle of claim 1, wherein the outer polymeric coating comprises a polyester.

7. The polymer-coated therapeutic nanoparticle of claim 1, wherein the outer polymeric coating comprises a biodegradable polymer.

8. The polymer-coated therapeutic nanoparticle of claim 6, wherein the polyester comprises Poly(ϵ -caprolactone) (PCL).

9. The polymer-coated therapeutic nanoparticle of claim 1, wherein the inner core is rod-shaped.

10. The polymer-coated therapeutic nanoparticle of claim 1, wherein the at least one therapeutic agent comprises an anti-cancer agent.

11. The polymer-coated therapeutic nanoparticle of claim 1, wherein the maximum dimension of the inner core is between 100 nm and 200 nm.

12. The polymer-coated therapeutic nanoparticle of claim 1, wherein the outer polymeric coating entirely coats the inner core.

13. The polymer-coated therapeutic nanoparticle of claim 1, wherein at least a portion of the outer polymeric coating is configured to at least partly degrade, thereby releasing the at least one therapeutic agent.

14. A method for producing a polymer-coated therapeutic nanoparticle, the method comprising:

forming an inner core comprising at least one therapeutic agent, the inner core having a maximum dimension of 300 nm or less;

coating, at least partly, the inner core with a layer of a bio-responsive polymer, the layer of the bio-responsive polymer having a thickness of 1 nm to 100 nm; and attaching at least one targeting molecule to the layer of the bio-responsive polymer.

15. The method of claim 14, wherein the forming the inner core and the coating, at least partly, the inner core comprises utilizing a solvent diffusion method.

16. The method of claim 15, wherein the at least one therapeutic agent and the bio-responsive polymer are simultaneously added to an aqueous solution.

17. The method of claim 14, wherein the attaching at least one targeting molecule comprises covalently bonding the at least one targeting molecule to the layer of the bio-responsive polymer.

18. The method of claim 14, further comprising modifying the layer of the bio-responsive polymer prior to the attaching at least one targeting molecule.

19. A polymer-coated therapeutic nanoparticle comprising:

a rod-shaped inner core comprising an anti-cancer therapeutic agent, wherein the rod-shaped inner core has a maximum dimension of 450 nm or less;

an outer polymeric coating at least partly covering the rod-shaped inner core, wherein the outer polymeric coating has a thickness from 1 nm to 100 nm, and wherein the outer polymeric coating comprises a bio-responsive polymer; and

at least one targeting molecule covalently attached to the outer polymeric coating, wherein the at least one targeting molecule comprises a polypeptide.

20. The polymer-coated therapeutic nanoparticle of claim **19**, wherein the polypeptide comprises an antibody.

* * * * *